

PAPER • OPEN ACCESS

Thermodynamic effects in a gas modulated Invar-based dual Fabry–Pérot cavity refractometer

To cite this article: T Rubin *et al* 2022 *Metrologia* **59** 035003

View the [article online](#) for updates and enhancements.

You may also like

- [The influences of different filler metals on the microstructure of Invar Fe-36Ni alloy multi-layer multi-pass MIG welding](#)
Xiaohong Zhan, Zhenxin Zhu, Tingyan Yan et al.
- [Investigations on density and surface roughness characteristics during selective laser sintering of Invar-36 alloy](#)
Navneet Khanna, S Mistry, R A Rahman Rashid et al.
- [Electrodeposition of Invar Fe-Ni Alloy/SiC Particle Composite](#)
Tomio Nagayama, Takayo Yamamoto and Toshihiro Nakamura

Thermodynamic effects in a gas modulated Invar-based dual Fabry–Pérot cavity refractometer

T Rubin^{1,*}, I Silander², J Zakrisson², M Hao³, C Forssén^{2,4},
P Asbahr¹, M Bernien¹, A Kussicke¹, K Liu³, M Zelan⁴
and O Axner²

¹ Physikalisch-Technische Bundesanstalt (PTB), Abbestr 2-12, Berlin, Germany

² Department of Physics, Umeå University, SE-901 87 Umeå, Sweden

³ School of Mechanical Engineering and Automation, Northeastern University, NO. 3-11, Wenhua Road, Heping District, Shenyang, People's Republic of China

⁴ Measurement Science and Technology, RISE Research Institutes of Sweden, SE-501 15 Borås, Sweden

E-mail: Tom.Rubin@PTB.de

Received 13 October 2021, revised 19 January 2022

Accepted for publication 17 March 2022

Published 14 April 2022



Abstract

By measuring the refractivity and the temperature of a gas, its pressure can be assessed from fundamental principles. The highest performing instruments are based on Fabry–Pérot cavities (FPC). Gas modulation refractometry (GAMOR) is a methodology that has the ability to reduce the influence of disturbances to such an extent that high-precision (sub-parts-per-million) assessments of pressure can be made by the use of FPCs of Invar. To allow for high accuracy assessments, it is of importance to assess the uncertainty contribution from the thermodynamic effects that are associated with the gas filling and emptying of the cavity (pV -work). This paper presents a detailed scrutiny of the influence of the gas exchange process on the assessment of gas temperature on an Invar-based dual-FPC (DFPC) instrumentation. It is shown that by virtue of a combination of a number of carefully selected design entities (a small cavity volume with a bore radius of 3 mm, a spacer material with high heat capacitance, large thermal conductivity, and no regions that are connected with low thermal conductance, i.e. no heat islands, and a continuous assessment of temperature of the cavity spacer) the system is not significantly affected by pV -work. Simulations show that 10 s after the filling all temperature gradients in the system are well into the sub-mK range. Experiments support that refractivity assessments initiated after 40 s are not significantly affected by the pV -work. The analysis given in this work indicates that an upper limit for the influence of pV -work on the Invar-based DFPC system using 100 s long gas modulation cycles is 0.5 mK/100 kPa (or 1.8 ppm/100 kPa). Consequently, thermodynamic effects will not be a limiting factor when the Invar-based DFPC GAMOR system is used for assessments of pressure or as a primary pressure standard up to atmospheric pressures.

Keywords: quantumpascal, GAMOR, optical pressure standard, gas refractometry, pV -work, Invar-based

(Some figures may appear in colour only in the online journal)

* Author to whom any correspondence should be addressed.



Original content from this work may be used under the terms of the [Creative Commons Attribution 4.0 licence](https://creativecommons.org/licenses/by/4.0/). Any further distribution of this work must maintain attribution to the author(s) and the title of the work, journal citation and DOI.

1. Introduction

Fabry–Pérot cavity (FPC) based refractometry is a sensitive laser-based methodology for the assessment of molar density and pressure [1–7]. By measuring the refractivity, $n - 1$, where n is the index of refraction, the density of a gas can be calculated using the Lorentz–Lorenz equation, and, if also its temperature is known, its pressure can be assessed by an equation of state [8–13]. The technique has demonstrated assessment of molar densities and pressures with both high precision and good accuracy over a large dynamic range (for pressure, ranging from low mPa to hundred kPa). Recent works have indicated that the methodology also has the potential to replace current pressure standards, in particular in the 1 Pa to 100 kPa range [12–16].

To be able to assess pressure with highest accuracy, which is of particular importance if it is to be used as a primary standard, it is of importance to make use of accurately assessed gas parameters and utilize well calibrated temperature sensors or fixed points. The relevant gas parameters are the molar polarizability and the refractivity and density virial coefficients of the gas under scrutiny. It is also of importance to certify that the assessments are taken under adequate conditions; in particular to assess whether the gas exchange process affects the assessment of the gas temperature [17].

If a volume of gas is flowing from a region with higher pressure to one with lower, the gas particles will be accelerated along the streamline, experiencing a net force driven by the pressure difference in the two volumes. This implies that the gas species entering the low pressure compartment can have speeds that are significantly larger than both the mean thermal velocity of the gas originally residing in the cavity and the speed of sound. Hence, the gas brings in excess energy into the ‘low’ pressure compartment. The gas transferred into this compartment will then, by mutual collisions, increase the mean thermal velocity of its species, which is tantamount to that its temperature increases. The entering gas species will similarly interact with the walls of the compartment and will heat those up as well. The energy for both these processes is taken from the gas species in the high pressure compartment, whose temperature thus decreases. This takes place even if the gas is ‘ideal’. Since this will influence the temperature distribution in the system (both the temperature of the gas and the cavity spacer), it can have an adverse influence on the ability of the system to correctly assess the pressure.

A thorough investigation of this effect on the fixed length optical cavity (FLOC) system at NIST (National Institute of Standards and Technology, USA) was recently carried out by Ricker *et al.* [17]. It was concluded that the filling of gas in their system will affect the cavity temperature homogeneity for a considerable amount of time, impeding the ability to measure the gas temperature with highest accuracy, which, in turn, adversely affects the ability to use the system as a primary standard for pressure. The results from modelling presented in that paper showed that, when the measurement cavity was filled with gas (from 1 kPa to 100 kPa), the temperature of various parts of the system (defined as the glass elements of

the refractometer and the ‘thermal-shell’ copper chamber) is homogeneous to within 0.5 mK only after an equilibration time of 3000 s. If cavity materials are used, that are permeable for the gas (e.g. ULE glass combined with helium and other gases) then the important purity of the gas is at higher risk for longer equilibration times [18]. In general such a long equilibration time precludes rapid assessments and opens up for the risk to be significantly influenced by drifts [19].

The gas modulation refractometry (GAMOR) methodology, which previously has demonstrated an outstanding ability to mitigate the influence of disturbances (predominantly fluctuations and drifts), utilizes gas modulation cycles in the order of 100–200 s [15, 20–24]. In order for such systems to provide accurate assessment, it is of importance to ascertain that they are not significantly affected by temperature effects caused by the exchange of gas on this time scale.

Since the Invar-based dual-FPCs (DFPCs) system used with the GAMOR methodology has a dissimilar construction as compared to the NIST-FLOC system, it is not directly possible to draw conclusions from the work by Ricker *et al.* [17] regarding properties of the Invar-based GAMOR system. On the other hand though, it is possible to conclude that since it originally was constructed to facilitate gas exchange processes, there are indications that it is not strongly affected by thermodynamic effects from gas exchange processes; in fact, it has been tacitly assumed that the influence of pV -work on assessments of pressure in the Invar-based GAMOR system is significantly smaller than what it is in the NIST-FLOC system and that it is insignificant on the time scales of the gas modulation. So far, however, this assumption has not been verified.

The most prominent reasons why the Invar-based FPC-system is not expected to be strongly affected by thermodynamic effects are the following ones [25, 26]. The cavity system used is ‘closed’, implying that the gas does not fill a volume surrounding the spacer like for an ‘open’ system. Instead the gas fills only one of the cavities. Each cavity has been manufactured with a thin bore (with a radius of 3 mm). This implies that the gas rapidly takes the temperature of the cavity wall (within a fraction of a second) and that each filling of gas brings in only a small volume of gas (with a spacer length of 148 mm, $<5 \text{ cm}^3$), and thereby only a small amount of energy. Invar has a high volumetric heat capacity, which implies that a given amount of energy (supplied by the gas) only provides a small temperature increase in the spacer material. The fact that Invar also has a high thermal conductivity and that the system has been constructed without any heat islands (i.e. regions that are connected with low thermal conductance) imply that any small temperature inhomogeneity rapidly will spread in the system (significantly faster than in systems with cavity spacers made of glass materials or with larger gas volumes). Moreover, since the temperature of the cavity spacer is assessed by the use of sensors either placed in holes drilled into the cavity spacer (three Pt-100) or wrapped around the outside of the spacer (a thermocouple) whose output is referred to a gallium fix point cell, the assessment of gas temperature is not affected by any possible homogeneous heating of the cavity spacer; it is only influenced by the difference between the

temperature of the cavity spacer at the position(s) of the sensors and that of the cavity wall. All this points to the fact that the Invar-based DFPC system is not significantly affected by thermodynamic processes associated with the filling and evacuation of gas, which allows for the rapid gas exchanges that are utilized in the GAMOR methodology.

To assess whether the Invar-based DFPC GAMOR system is affected by such processes, and if so, to which degree, this work presents, by both simulations and experimental assessments, a detailed scrutiny of the influence of the gas exchange process on its assessment of gas temperature (and thereby pressure).

2. Theory

2.1. Thermodynamic estimates

When gas is transferred from a pressurized volume into an evacuated one, work is carried out that leads to an increase in its temperature. Baker showed that this work can be estimated by considering the reverse process (i.e. a filling process) at constant pressure [27]. The work done on a gas that flows out of a vessel when its volume is reduced can be estimated by considering a piston with an area A that moves a distance l in a tube as $W = \int_0^l pA \, ds = pV = Nk_B T$, where N is the number of gas molecules and T the initial temperature.

The gas takes its maximum temperature in the fictitious case when no energy is transferred to the surrounding walls. In this case, all the work performed by the piston contributes to the internal energy of the gas, ΔU , which, if distributed among all degrees of freedom of the gas species, f_U , is given by $\frac{f_U}{2} Nk_B \Delta T$, where ΔT is the increase in temperature. This shows that the maximum increase in temperature the gas can experience is given by $\Delta T = \frac{2}{f_U} T$. For nitrogen (for which $f_U = 5$) at an initial temperature of 300 K the theoretical maximal temperature increase, when the entire internal energy of the gas is distributed among all degrees of freedom of the gas species, for a homogeneously distributed temperature, is 120 K.

For the more realistic case when the gas also transfers energy to the walls, the increase in gas temperature will be lower (although the total energy transferred to the originally evacuated vessel is the same). This was experimentally verified by Jousten for a situation in which helium as well as argon were expanded from a small constant volume vessel with pressures between 30 and 300 kPa into a larger evacuated one [28].

Irrespective of which peak temperature the gas reaches during this process, the gas will inevitably, by collisions with the cavity walls, rapidly thermally equilibrate with the cavity walls whereby all of the associated energy eventually will be transferred to those. It can be estimated from gas dynamic considerations that, for the narrow bore system scrutinized in this work, and under sub-atmospheric or atmospheric pressure conditions, this should take place at a sub-second time scale.

The energy delivered by the gas to the cavity material, which for a system with a tiny volume is small (<0.5 J for

a system with a volume <5 cm³ filled to atmospheric pressure), will diffuse into the spacer material according to the equation of heat. The characteristic time scale for this depends on the geometry of the cavity spacer, the thermal conductivity of the spacer material, and the presence (or absence) of any possible heat islands. For the Invar-based DFPC system under scrutiny here, the characteristic time scale for this process can be estimated to be in the few or ten seconds range. This implies that, at the time when the refractivity assessments are being made, which normally takes place 40–50 s after the initiation of the filling of gas, any spatially inhomogeneous temperature distribution in the cavity spacer material caused by the introduction of gas is expected to have decayed several orders of magnitude (typically to sub-mK levels). Consequently, the Invar-based DFPC system utilizing the GAMOR methodology is not expected to be significantly affected by thermodynamic processes that are associated with the exchange of gas.

These estimates are supported by simulations presented in section 4 and verified by cycle-resolved measurements shown in section 5.

2.2. Refractometry and GAMOR

GAMOR-based refractometry is based on the same fundamental principle as ordinary (unmodulated) FPC-based refractometry; it measures the change in refractivity between two situations, with and without gas in a cavity (henceforth referred to as the measurement cavity), as a change in the frequency of laser light that is locked to a mode of the cavity. Moreover, for best stability, it has so far been implemented in DFPC systems. This implies that the change in refractivity, in practice, is assessed as a shift in the beat frequency between the frequencies of two lasers, one addressing the measurement cavity and one probing the reference cavity when gas is let into (or evacuated) from the measurement cavity [15, 20, 22–24].

Assessment of gas refractivity from the measured shift in beat frequency, both for refractometry in general and the GAMOR methodology specifically, are made by the conventional means, as has been described in the literature [29]. The assessments of gas density and pressure from gas refractivity have likewise been given in the literature [8, 11, 21, 29–31].

3. Experimental

The Invar-based DFPC-refractometer used in this work is, to a large extent, identical to the one presented in detail in some other publications [15, 25, 26]. The heart of the system is the cavity spacer, which is machined from a rod of Invar (see figure 1). In the spacer, two throughgoing holes for the measurement and reference cavities, and three likewise throughgoing holes for temperature sensors (seen on the short end and on the top of the cavity assembly, respectively) have been drilled. In the middle of each cavity, a vacuum tube is connected from the side in order to either supply the cavity with gas or evacuate it. To mount the cavity mirrors to the spacer the mirrors are placed in a machined inset with O-rings pressing against the back of the mirror substrates. Vacuum tight seals are obtained by pressing the mirrors, via the O-rings, by

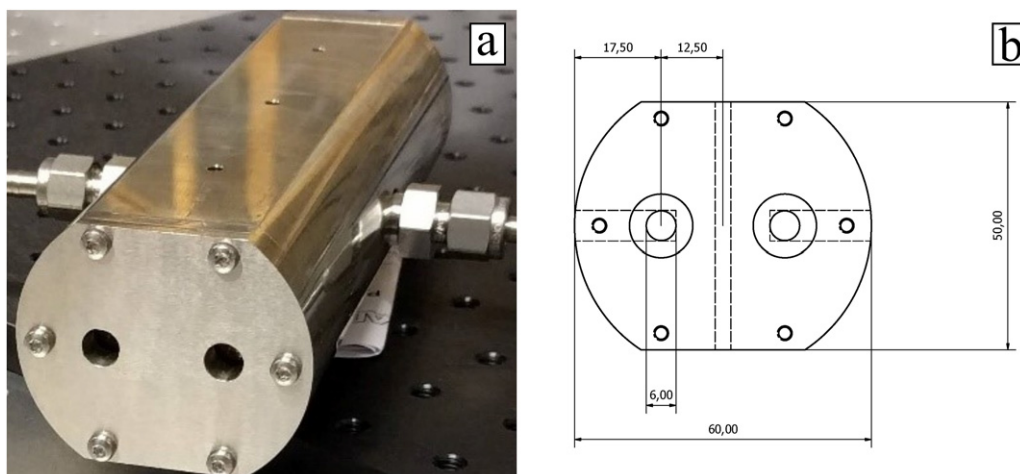


Figure 1. Panel (a): the Invar cavity assembly before being equipped with temperature sensors and mounted inside the aluminium oven. The plates screwed into the spacer at its short ends press the mirrors, via O-rings, onto the spacer. Panel (b): a schematic drawing of the cavity assembly. Units in mm. Reproduced from [32]. © The Author(s). Published by IOP Publishing Ltd. [CC BY 4.0](#).

plates (with the same cross section as the cavity spacer) that are screwed onto the spacer.

The cavity spacer is placed in an aluminum enclosure (referred to as the oven) and is supported by four sharp pegs at the points of minimum deflection. By this, all thermal bridges to the spacer are minimized ensuring that the spacer is heated uniformly by the air inside the oven. On top of the oven, four pneumatic vacuum valves, used to control the flow of gas via vacuum tubing to and from the cavities, are mounted. This ensures that the temperature of the valves and tubing leading into the cavity spacer will follow that of the oven.

The temperature stabilization of the spacer is performed in three stages. In the first, the measurement environment, i.e. the box that houses the refractometer, is stabilized to be within 100 mK of the melting point of gallium, T_{Ga} (302.9146 K), by heating the covered breadboard on which the setup is mounted.

In the second stage, the temperature of the oven is measured with a Pt-100 sensor inserted in the bottom of the oven. This temperature reading is used to apply feedback to four Peltier elements, placed under the oven, that regulate the oven temperature with respect to the set temperature.

In the third stage, the temperature of the cavity spacer, measured as the mean of three Pt-100 sensors that are inserted into the cavity spacer, T_{cav} , is used to apply feedback to the set point of the oven servo stage. This feedback aims at keeping the spacer at the Ga melting point. After the feedback is engaged, the temperature of the cavity spacer stabilizes within 1 mK of T_{Ga} within 3 h.

The cavity temperature can be assessed with either three Pt-100 sensors or by a thermocouple referred to a gallium fix point cell [26]. When the Pt-100 sensors are used, the temperature of the cavity spacer is assessed by measuring the resistance of the three sensors mounted in the spacer holes by a temperature input module (National Instruments, NI-9216). When the Ga fix point cell is used, the temperature difference between the Ga sample and the spacer is measured by the use of a type-T

thermocouple wound around the cavity spacer. As the difference in temperature is small this voltage is typically in the μV range and is assessed by a nanovoltmeter (Keithley, 2182A).

The expanded long term (40 days) uncertainties of the temperature assessment performed by the Pt-100 sensors and the thermocouple referred to the fix point cell have been assessed to 7.8 mK and 1.2 mK, respectively [15]. However, although the thermocouple has a lower uncertainty (better accuracy) than the Pt-100 sensors, it has a larger level of (short term) noise. It is therefore not the best choice for cycle-resolved assessments. On the other hand, on short time scales, i.e. 10 h, the difference between the two methods has been shown to be within a fraction of a mK (for $k = 2$, within 220 μK) [26]. This implies that, for cycle-resolved assessments, it is advisory to assess temperature fluctuations by use of the Pt-100 sensors.

Figure 2 shows a schematic view of how the refractometer is connected to the gas system, comprising a common gas supply and distribution system. In the figure, the colored lines represent gas lines where the red color relates to low pressures while the blue one represents high pressures.

The gas modulation cycle is achieved by switching between state I and II, which are shown in the insert in figure 2. During the gas filling and stabilization stage (state I), the valves 2 and 3 are closed, while the valves 1 and 4 are open, resulting in evacuation of the reference cavity (represented by the red gas lines). During the evacuation stage (state II), the valves 1 and 3 are closed, while the valves 2 and 4 are open, resulting in evacuation of the both cavities.

To be able to experimentally characterize this system, we have utilized a dead weight piston gauge (DWPG) to create and maintain a pressure that can be assessed by the refractometer.

To fill the system with gas, the gas supply system, consisting of a mass flow controller (MFC, Bronkhorst, FG-201CV) and an electronic pressure controller (EPC Bronkhorst, P-702CV), is connected to a central gas distribution system (in this work distributing N_2). Referring to figure 2, in the volume to the left of valve 5, gas constantly circulates to

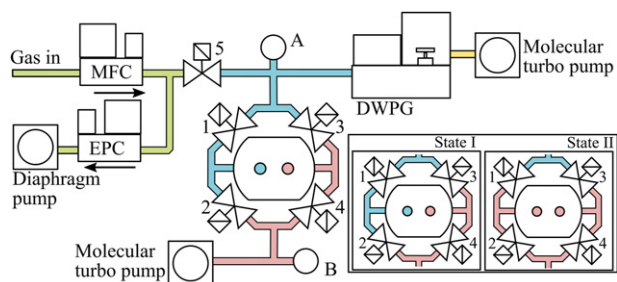


Figure 2. Schematic illustration of the gas supply-and-evacuation system. Different parts of the gas lines are indicated by colors: green: the supply part; blue: the high pressure part; red: the low pressure part; and yellow: the DWPG hood pressure. A and B represent pressure gauges. MFC: mass flow controller; and EPC: electronic pressure controller; DWPG: dead weight piston gauge. The insert shows the two valve states: state I: gas filling and stabilization stage; and state II: the evacuation stage.

prevent contamination from building up. Valve 5 is opened and closed by a relay that is controlled by the pressure measured by gauge A (Oerlikon-Leybold, CTR 101 N 1000 Torr). Whenever the reading of pressure gauge A falls below a user-defined set-pressure valve 5 opens, re-filling the system. After the filling, the valve will close, whereby the DWPG will automatically regulate the pressure to its set-pressure (by changing the volume).

Although the GAMOR methodology normally is performed with gas modulation cycles with a cycle time of 100 s, to more clearly assess a possible drift of the signal caused by any pV -work, a series of simulations and measurements were in this work made for a variety of pressures of nitrogen with gas modulation cycles with a cycle time of 200 s (distributed over a 100 s filling-and-stabilization part and a 100 s evacuation part).

4. Simulations

Let us first emphasize that the DWPG is not a part of the Invar-based DFPC refractometer; it is used solely to produce a pressure that the refractometer can assess under various conditions. Hence, to assess the inherent properties of the refractometer, all simulations were carried out without taking the finite response time of the DFPG into account.

The simulations considered the filling of one cavity in a DFPC system, denoted the measurement cavity, while the other was held at vacuum. For simplicity, the simulations were made in two consecutive steps. The first one addressed the gas dynamic processes that take place in the cavity when nitrogen is let into an empty cavity while the second one dealt with the heat transport (and distribution) processes in the cavity spacer. As is shown below, the simulations indicate that the equilibration of pressure in the cavity takes place on a time scale of tens of ms while the temperature of the gas equilibrates with that of the cavity walls on a time scale of a second. They also indicate that the subsequent diffusion of heat in the spacer material takes place on a time scale of ten seconds. The fact that the gas dynamic effects take place on a time scale that is more than one order of magnitude shorter than the heat transport processes in

Table 1. Parameters and conditions of the simulations of the development of the gas pressure and temperature in the measurement cavity.

Parameters	Value
Gas species	Nitrogen
Initial pressure	0 kPa
Wall temperature	302.915 K
Wall interaction	'No slip'
Gas temperature at the inlet	302.915 K
Inlet pressure	30 or 100 kPa
Length of time step during the first 10 μ s	1 μ s
Length of time step during the subsequent 0.50 s	50 μ s
Length of time step during the following 0.75 s	500 μ s
Length of time step during the last 0.75 s	5000 μ s

the spacer justifies the separation of the thermodynamic effects in the system into two consecutive steps—gas dynamics and spacer thermalization.

4.1. Gas dynamics—pressure and thermal equilibration of the gas after introduction into the cavity

The pressure and temperature equilibration processes in the measurement cavity were simulated using the Ansys software version 16.0 together with the included fluid dynamics tool Fluent 16.0. Two different conditions were simulated; 30 kPa of nitrogen let into the measurement cavity (representing one of the cases studied experimentally, see below, referred to as case 1), and 100 kPa (representing atmospheric pressure conditions, case 2). Since the cavity spacer is held at the melting point of gallium (302.915 K), the wall temperature of the cavity was assumed to be the same. Moreover, since the cavity has a volume that is similar to that of the gas lines prior to the gas regulating valve (valve 1 for the measurement cavity) inside the housing box, it has been assumed that also the temperature of the gas when it enters the cavity is at the Ga melting point. The conditions used for the simulations are summarized in table 1. To simplify the simulations, the boundary conditions used were that the temperature of the cavity wall is kept constant (due to its minor temperature fluctuations) and that the inlet pressure is reached instantaneously.

Figure 3 shows the 3D-CAD model of the DFPC resonator that was used for finite-volume method simulations with Ansys. To shorten the computation time, and due to symmetry reasons, only one half of the cavity (length-wise) was simulated. Although the temperature and pressure fluctuations were evaluated at all grid points of the 3D model, five so called 'monitoring points' as well as the center line of the cavity were chosen for in depths observations of the system. The five points, marked by the red points in figure 3, are positioned in the center of the measurement cavity (i.e., with $x = -12.5$ mm and $y = 0$ mm). They are arranged equidistantly between point 1, which is at the gas inlet, and point 5, which is half a millimeter away from one of the cavity mirrors. Consequently, the z -positions for five points (from 1 to 5) are: 0, 18.5, 37, 55.5, and 73.5 mm, respectively. The thin, solid line represents the center part of the cavity that is probed by the laser light.

Figure 4(a) shows, by the lower (solid) and upper (dashed) sets of colored curves, the time development of the pressure for

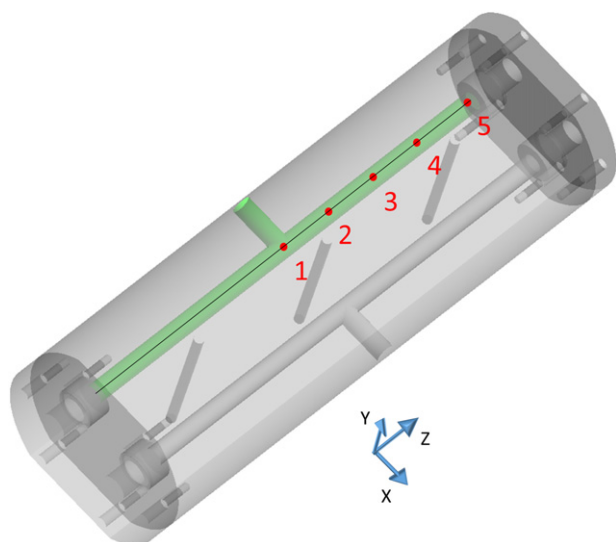


Figure 3. Schematic drawing of the DFPC spacer. The cavity illustrated in green is the measurement cavity, which is filled with gas during in the beginning of each modulation cycle. The five red points indicate the positions of the five monitoring points in the simulation. The thin, solid line represents the center part of the measurement cavity that is probed by the laser light. The three bores along the y-axis between the cavities are where the Pt-100 sensors are inserted.

the first 10 ms at the five monitoring points after the introduction of 30 and 100 kPa of nitrogen into an empty measurement cavity held at the gallium melting point, respectively. The solid and dashed black curves indicate their averages along the center of the cavity (the solid line in figure 3, representing the part of the gas that is probed by the laser light).

Panel (b) illustrates, by the five colored curves, the temperature of the gas at the five monitoring points for the first 2 s after the introduction of 30 kPa of gas. Again, the solid black curve represents their average along the center-line of the cavity. The dashed black curve illustrates the corresponding average for 100 kPa. Note the difference in scales of the x-axes; while panel (a) illustrates the pressure over the first 10 ms, panel (b) shows the temperature during the first 2 s.

Panel (c) finally, displays, by the solid and the dashed curves, the time development of the difference between the average temperature of the center part of the cavity (i.e. the part of the cavity probed by the laser light) and the fixed temperature of the cavity wall for the first 2 s when 30 kPa or 100 kPa are introduced, respectively.

Panel (a) shows that, after the introduction of gas, for both pressures, the pressure in the cavity equilibrates rapidly (within 10 ms). Panel (b) shows, on the one hand, that the maximum increase in the (average) temperature of the gas that is probed by the laser is 20 and 50 K for the cases with 30 and 100 kPa, respectively, but also, on the other hand, that this increase in temperature rapidly decays (on a sub-second time scale).

Panel (c) illustrates, by the solid curve, that when 30 kPa of nitrogen is let into the cavity, the average temperature of the part of the cavity that is probed by the laser light (the center part of the cavity) decays towards the cavity wall temperature

in an exponential manner with a time constant of 0.07 s. It also shows that it is within 1 mK of the temperature of the wall after around 1 s (after 1.05 s).

The dashed set of data indicates that when 100 kPa of nitrogen is introduced the decay is slightly slower; the gas temperature decays exponentially towards the cavity wall temperature with a time constant of 0.14 s and it is within 1 mK of the temperature of the wall after 1.5 s.

4.2. Thermalization of the cavity spacer

The transport and distribution of heat in the cavity spacer were simulated with the FEM-software: COMSOL Multiphysics® (version 5.4) assuming that an amount of energy of 0.15 J (representing the pV -work from a gas at a pressure of 30 kPa) is deposited by the gas to the cavity walls. To take gas dynamic effects into account, the energy was deposited in an exponentially decaying manner with a time constant given by the longest decay displayed in figure 4(b), i.e. 0.14 s. The conditions used for the simulation are summarized in table 2, where the mirrors were simulated using a standard glass type (N-BK7).

Figure 5 shows some typical results of such simulations for a few selected time instants, displayed as heat maps of a cross section of the Invar spacer at the z -position of the first Pt-100 sensor (i.e. at 50 mm from the center of the cavity) in a 200 s long gas modulation cycle when 30 kPa is let into the measurement cavity. The upper row of heat maps represents the first hundred seconds of the gas modulation cycle (i.e. the gas filling and stabilization part of the cycle), while the lower one depicts the second hundred second section of the modulation period (representing the evacuation stage). The black circular areas in the panels represent the cavity bores while the black curves outline the outer surface of the cavity spacer. The domains outside the black curves comprise air whose outer boundaries have a fixed temperature.

The simulations show, first of all, that for the case considered, the energy deposited by the gas will cause heating of the cavity spacer solely in the low or sub-mK range. The maximum heating any part of the cavity spacer will experience after 1 s is <5 mK, which is more than four orders of magnitude smaller than the theoretically maximum heating of the gas, calculated as pV .

The upper row of heat maps also shows that the heat will thereafter rapidly (on the scale of seconds) diffuse into (and distribute within) the cavity spacer; e.g. after 10 s, the temperature of the cavity spacer has, at no point, increased more than 1 mK, and, after 30 s, which is well ahead of the time when the refractivity assessments are made (which, under normal working conditions, i.e. when gas modulation periods of 100 s are used, takes place 40–50 s after the filling of gas, and, in this work, when 200 s long modulation periods are utilized, takes place after 90–100 s), the maximum temperature increase is well into the sub-mK range. The lower row of heat maps shows that a similar situation takes place during the evacuation, with a corresponding decrease of the temperature. After 200 s the spacer temperature is equilibrated within 0.1 mK from the original temperature.

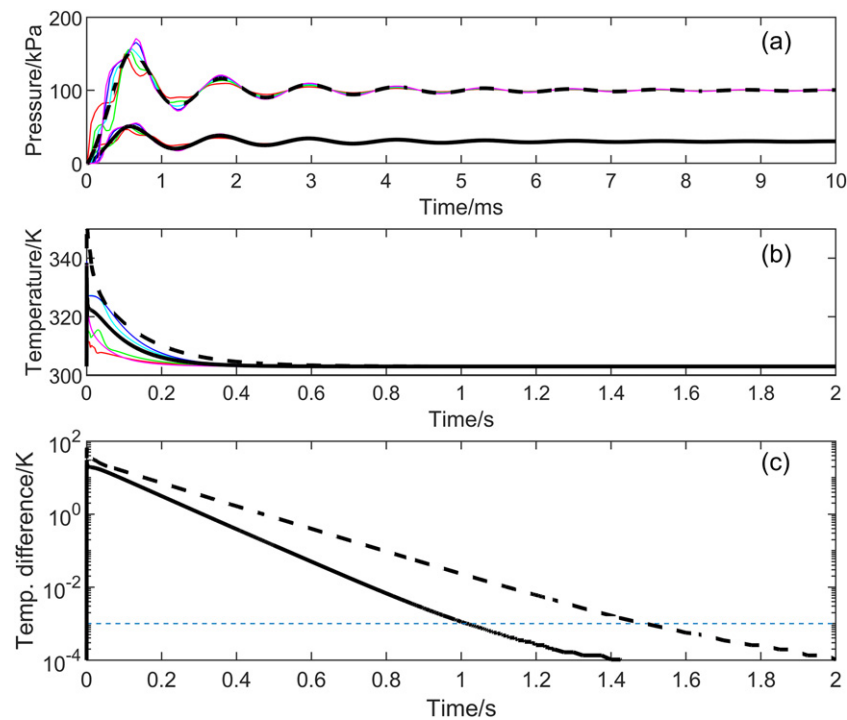


Figure 4. Panel (a) shows the time development of the pressure in the measurement cavity at the five monitoring points (1: red; 2: green; 3: cyan; 4: blue; and 5: magenta) for the first 10 ms when nitrogen was introduced into the cavity. The lower and upper sets of colored curves represent the cases when 30 and 100 kPa were let into the cavity, respectively. The black solid and dashed curves denote the average along the center-line of the cavity. Panel (b) displays, by the colored curves, the time development of the temperature at the same five points when 30 kPa is introduced held at the gallium melting point. The solid curve illustrates the average of the temperature of the gas along the center-line of the cavity (i.e. the part of the cavity probed by the laser light). The dashed black curve shows the corresponding average for the case when 100 kPa is let in. Panel (c) shows, by the solid and the dashed curves, the time development of the difference between the part of the cavity probed by the laser light and the cavity wall when a pressure of 30 and 100 kPa of nitrogen is let into the cavity, respectively. The dashed blue line indicates a temperature difference of 1 mK.

Table 2. Parameters and conditions of the simulations of thermalization of the cavity spacer.

Parameters	Value
Material	Invar
Thermal conductivity	13.5 W m ⁻¹ K ⁻¹
Specific heat capacity	515 J kg ⁻¹ K ⁻¹
Density	8.15 g cm ⁻³
Initial temperature	302.915 K
Time steps	200 μs
Duration of gas modulation cycle	200 s
Gas filling and stabilization	0–100 s
Gas evacuation	100–200 s
Surrounding air pressure	1013 hPa
z-position	50 mm

The spatial and temporal distribution of heat is similar at other cross sections. For the case with 100 kPa (not shown), the heating and cooling of the spacer will be 3.3 times larger than illustrated in figure 5. It is notable though that, after 30 s, it is still in the sub-mK range.

To more clearly visualize the transport and distribution of heat in the cavity spacer, figure 6 shows the temperature deviation along the x -axis of the Invar-spacer in the middle of the cavity (i.e. at $\Delta y = \Delta z = 0$ mm) for the ten time instants displayed in figure 5. The green and the blue fields mark

the measurement and the reference cavity bores, respectively, while the gray areas represent the air outside the spacer.

The figure shows that while the temperature deviation close to the walls of the measurement cavity (i.e. at x_{m1} and x_{m2}) takes values in the low mK range for the first part of the gas modulation cycle (during the first few seconds), it reaches sub-mK values already after 10 s (and for times thereafter). At the center of the spacer (in between the two cavities), where the Pt-100 sensors are placed (i.e. at x_{Pt}), and at the rim of the spacer, where the thermocouple is placed (i.e. at x_{s1} and x_{s2}), the temperature deviation stays (for all times) in the sub-mK range. This demonstrates that the heat supplied (and subsequently removed) by the gas does not have any significant influence on the overall temperature of the cavity spacer; it has predominantly only a restricted temporal and spatial influence on the temperature distribution in the spacer that does not interfere with the temperature assessment (which is carried out as a cycle-averaged temperature at x_{Pt100} when the Pt-100 sensors are used and at x_{s1} and x_{s2} when the thermocouple is used).

4.3. Assessment of the temperature of the gas

It is of importance to note that since the GAMOR-based Invar cavity system is constructed with sensors that incessantly assess the temperature of the cavity, the assessment of pressure is not affected by any homogeneous steady-state heating

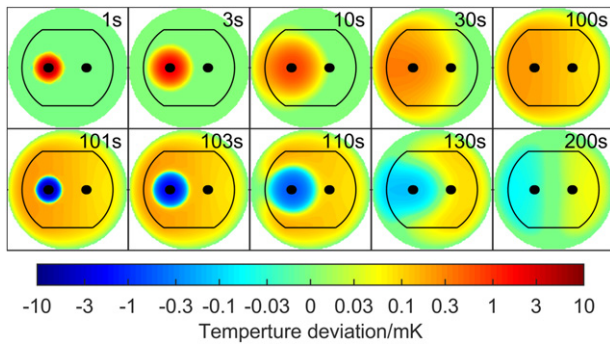


Figure 5. Time evolution of the temperature distribution of a full 200 s long gas modulation cycle, represented as heat maps of a cross section of the Invar spacer at the z -position of the first Pt-100 sensor (i.e. at a position 50 mm from the end of the cavity), when 30 kPa of nitrogen is introduced and evacuated from the measurement cavity. The first row of heat maps (1–100 s) corresponds to the filling of gas into the left cavity while the second row (101–200 s) depicts the subsequent evacuation. The black areas represent the cavity bores while the black curves outline the outer surface of the cavity spacer. The domain outside the black curve comprises air whose outer boundary has a fixed temperature (29.765 °C). Since the refractivity assessment when gas is present is performed between 90 and 100 s and the assessment when the cavity is empty between 190 and 200 s, the last heat maps in each row represent well the situations when the measurements are taken.

of the cavity spacer; it is only influenced by the difference between the temperature of the cavity spacer at the position(s) of the sensor(s) and that of the gas inside the cavity, which, for the given design, according to figures 4(b) and (c), almost instantaneously (i.e. within a fraction of a second) takes the temperature of the cavity walls. It is therefore of importance to monitor the temperature at a number of positions in the spacer.

Figure 7(a) illustrates the time development of the deviation of the temperature at seven different Δx positions in the cavity spacer at the Δy and Δz positions of one of the Pt-100 sensors (i.e. at $\Delta y = 0$ mm and $\Delta z = 50$) with respect to the temperature of the spacer before the initiation of the gas modulation procedure during the two first consecutive fillings and evacuations of 30 kPa of nitrogen in a series of gas exchanges. The seven curves represent the seven Δx positions marked in the upper part of figure 6. The dashed horizontal lines represent ± 0.3 mK, which correspond to ± 1 ppm.

The curves show that the increase in temperature that the measurement cavity initially experiences (which is out of scale in figure 7(a)) spreads, in due time, to all positions of the cavity spacer. However, they also show that, after 50 s, none of the monitored positions has increased its temperature more than 0.3 mK (1 ppm). The x_{m1} and x_{m2} curves additionally indicate that the temperature of the measurement cavity has been increased merely 0.26 mK after 50 s (given by the average of 0.22 and 0.28 mK) and 0.20 mK (the average of 0.18 and 0.22 mK) after 100 s.

It is important to emphasize though that when the temperature is assessed by use of the sensor(s), the assessments are likewise affected by the altered temperature at their positions. However, it has experimentally been found most reliable to average the measured temperature signal(s) over a

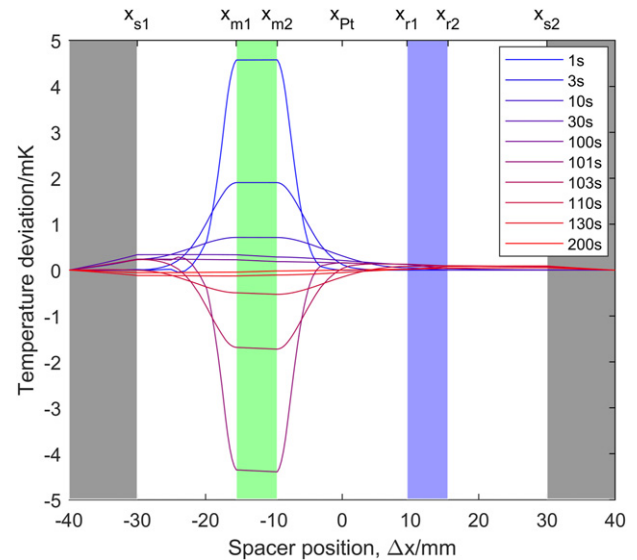


Figure 6. Temperature deviation along the width of the spacer (i.e. along a horizontal center line in the x -direction) at $\Delta y = \Delta z = 0$ mm for the ten time instances of the gas modulation cycle addressed in figure 5. Curve notations: 1–100 s represent the time after the introduction of gas while 101–200 s represent the following 100 s during the evacuation of the gas. All temperatures deviations are given with respect to the steady-state cavity temperature. The green and the blue fields represent the measurement and reference cavity bores, respectively, while the gray areas correspond to the air outside the spacer. Seven points of particular interest for the analysis are identified and marked at the upper x -axis. They represent: x_{s1} , the position of the leftmost outer surface of the spacer (at $\Delta x = -30$ mm); x_{m1} and x_{m2} , the left- and rightmost positions of the measurement cavity (at $\Delta x = -15.5$ and -9.5 mm); x_{Pt} , the position of the Pt-100 sensor (at $\Delta x = 0$ mm); x_{r1} and x_{r2} , the left- and rightmost positions of the reference cavity (at $\Delta x = 9.5$ and 15.5 mm); and x_{s2} , the position of the rightmost outer surface of the spacer (at $\Delta x = 30$ mm).

number of modulation cycles. This implies that the assessment of temperature is affected by an uncertainty that constitutes the difference between the spatially average temperature of the wall of the measurement cavity (x_{m1} and x_{m2}) and the time-averaged temperature at the positions of the sensor(s) (either as the average of the three x_{Pt} -positions or the average of x_{s1} and x_{s2}).

Based on panel (a), figure 7(b) therefore displays, by the red curve, marked Pt-100, the time development of the difference between the spatially average temperature of the measurement cavity wall and the time average of the temperature of the spacer at the positions of the three Pt-100 (the time average of three x_{Pt} curves of the type that is displayed in panel (a)) and, by the blue curve, marked TC, the time development of the difference between the spatially average temperature of the measurement cavity wall and the time average of the spatial average of the two positions at the outer surface of the spacer (i.e. the x_{s1} and x_{s2} curves) during a gas modulation cycle when addressing 30 kPa of nitrogen.

This implies that it is solely of importance what the difference between the temperature of the wall of the measurement cavity (which represents the gas temperature) and the time-averaged temperature of the spacer at the positions of the sensors is when the filled measurement cavity assessment is taken,

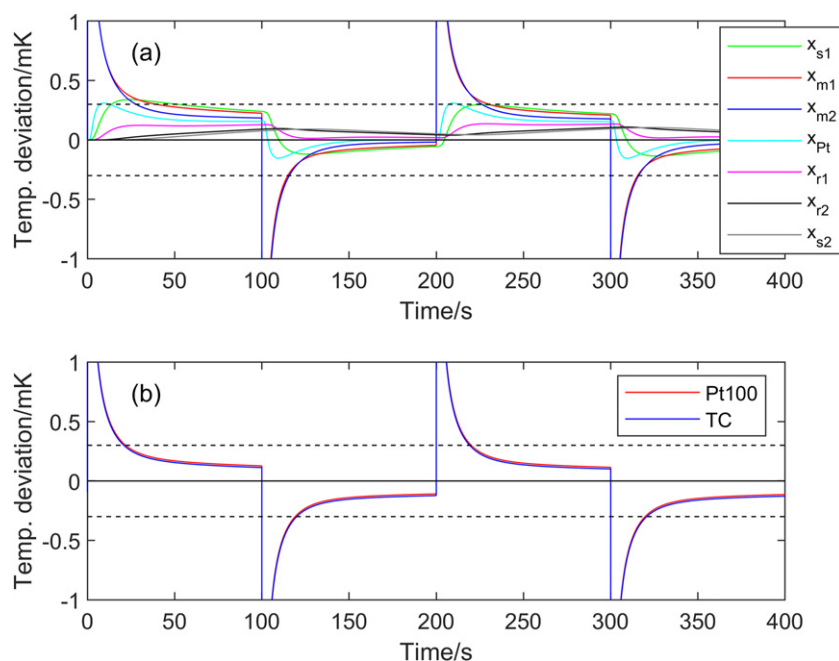


Figure 7. Panel (a). Time development of the deviation of the temperature at seven different Δx positions in the cavity spacer at the Δy and Δz positions of one of the Pt-100 sensors (i.e. at $\Delta y = 0$ mm and $\Delta z = 50$) with respect to the temperature of the spacer before the initiation of the gas modulation procedure during two consecutive 200 s long fillings and evacuations of 30 kPa of nitrogen. The seven curves show the temperature deviation at the seven Δx positions marked in figure 6. Panel (b). Time development of the temperature difference between the wall of the measurement cavity and the time-averaged temperature of the sensor positions; for the blue curve, marked Pt-100, the positions of the three Pt-100 sensors, and, for red curve, marked TC, those of the thermocouple after the filling of 30 kPa of nitrogen.

i.e. at the end of the gas supply-and-filling sections (for the situation displayed in figure 7, for the first modulation cycle between 90 and 100 s, and, for the second one, between 290 and 300 s); the temperature of the cavity wall when the measurement cavity is being filled or evacuated, or when the empty measurement cavity assessments are made, has no influence on a pressure assessment.

Figure 7(b) shows that the difference between the temperature of the wall of the measurement cavity and the time-averaged temperature of the sensor positions, 50 s into the supply-and-filling section, are 0.16 and 0.15 mK for the assessments by the Pt-100 and the thermocouples, respectively, and, after 100 s, 0.12 and 0.10 mK, for the same two sensors, respectively. Hence, when the filled measurement cavity refractivity assessments are made, the differences in temperature are, for the two types of sensors, when 100 s long modulation cycles are used, both within 0.5 ppm, and, when 200 s long modulation cycles are used, even below 0.4 ppm.

Taking into account that these numbers correspond to a pressure of 30 kPa implies that we can assess an upper limit for the influence of pV -work on the Invar-based DFPC system in its present configuration of, for 100 s long modulation cycles, 0.5 mK/100 kPa (1.8 ppm/100 kPa) and, for 200 s long cycles, 0.4 mK/100 kPa (1.3 ppm/100 kPa).

5. Experimental results

A series of measurements were performed for a variety of pressures of nitrogen in the 4–30 kPa range with gas modulation

cycles times of 200 s. Figure 8 displays, by the four pairs of panels, the 100 s long filling part of each cycle from four such pressures, viz 4.3, 10.2, 16.0, and 30.7 kPa.

The top panel in each pair shows the pressure settling process of the system as assessed by the refractometer. Each panel displays ten consecutive gas fillings, plotted as colored curves, while the solid black curve represents their average. The initial (15–20 s) parts of the data, which are out of scale, represent the combined effect of settling of the piston gauge and filling of the cavity. The dashed lines represent ± 3 ppm, which correspond to a variation (drift) of the temperature of ± 1 mK.

To assess the presence of any possible cycle-correlated temperature drift, the lower panel in each pair of panels shows, by the colored sets of data, the measured unaveraged temperature deviation of the same 10 modulation cycles expressed as the mean of the temperature of the three Pt-100 sensors located between the cavities. To enhance the assessment, the black curves in these panels represent the average of 100 consecutive such gas modulation cycles. In both cases, the deviations are expressed with respect to the mean value of the black (averaged) curves.

The x_{pt} curve in figure 7(a) above presented the simulated time development of the temperature of the spacer at the position of one of the three Pt-100 sensors. Of this data, the first 100 s correspond to the gas supply-and-filling section of the cycle. The latter part of this section predicts that the modulation-induced variation of the temperature of the spacer at the position of the Pt-100 sensor is below 0.3 mK. The figures 8(b), (d), (f) and (h) present the corresponding measured time evolution of the temperature deviations

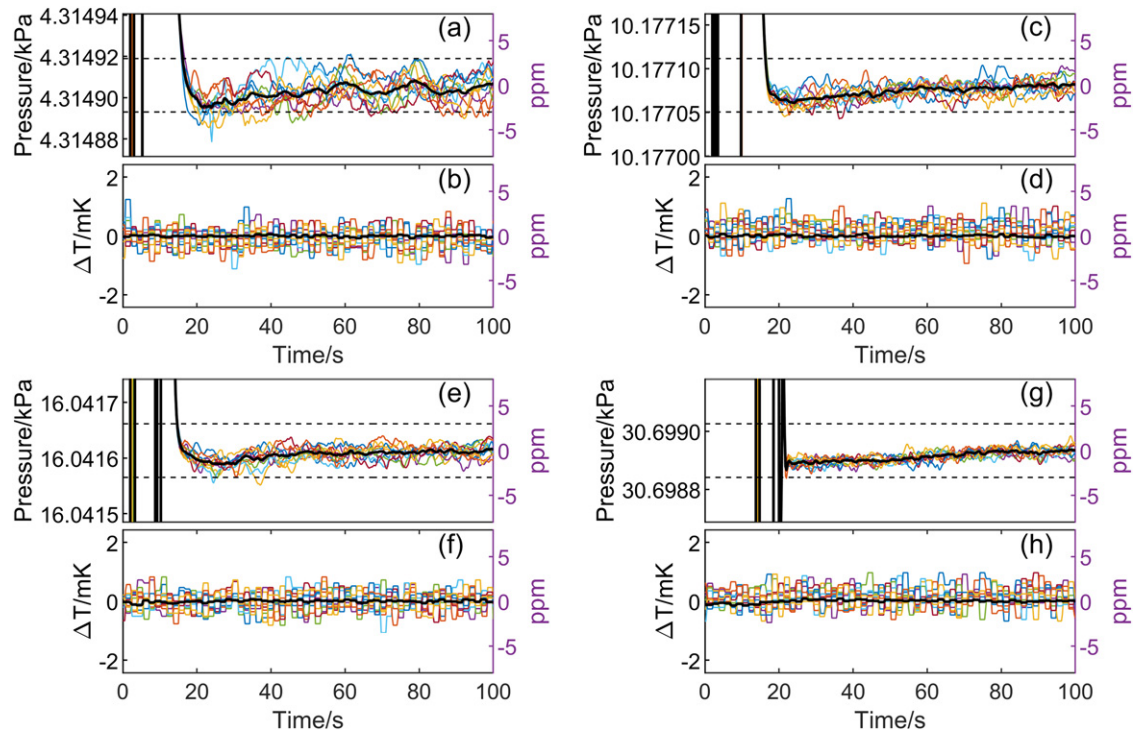


Figure 8. The upper panels in each pair of panels, i.e. the panels (a), (c), (e), and (g), display, by their coloured curves, the gas filling part (0–100 s) of 10 individual consecutive gas modulation cycles (each with a total modulation time of 200 s) for four different set pressures of the DWPG, viz 4.3, 10.2, 16.0, and 30.7 kPa. The black curves show the mean of the ten individual coloured curves. The dashed black curves represent ± 3 ppm deviations from the measured pressure. The lower panels in each pair, i.e. the panels (b), (d), (f), (h), illustrate, by the colored curves, the mean temperature of the three Pt-100 sensors in the cavity spacer during the same 10 cycles in terms of the average temperature of 100 consecutive temperature assessments of the three Pt-100 sensors. The black curves depict the mean of 100 consecutive temperature assessments normalized to their individual averages.

during the gas filling assessed as the mean of the three Pt-100 sensors. These measurements do not show, for any pressure, any modulation-correlated temperature variation. The reason for this is attributed to the finite resolution of the temperature measurement, which is similar to the simulated modulation-induced dependence. The lack of any clear modulation-correlated temperature dependence indicates that the simulations can be seen as an upper limit of the true temperature variation.

Since the Pt-100 sensors are closer to the gas modulated measurement cavity than the thermocouple, it can also be argued that it should be more strongly affected than the thermocouple by any modulation-induced temperature variation. Since the temperature variations at the Pt-100 sensors are too small to be resolved by the measurement system, it is likewise unlikely that there should be any detectable modulation-correlated fluctuations in the response of the thermocouple. This is in agreement with observations (not explicitly shown).

6. Analysis and discussion

The FLOC system developed by NIST was recently carefully scrutinized for its use as a primary temperature standard with respect to its response to the thermodynamic effects of gas exchanges [17]. The system was found to be adequate under the condition that it is given enough time to equilibrate after a

gas filling (in the order of 3000 s to reach an uncertainty level of 0.5 mK). The merits of the Invar-based DFPC system scrutinized in this work with respect to its response to pV -work can therefore most conveniently be estimated and appreciated by a comparison with that system.

6.1. Gas dynamics

Figure 4 shows that the pressure and temperature variations that originate from filling the cavity with gas can be substantial on the shortest time scales but also that they rapidly decay to an equilibrium. As was alluded to above, panel (a) shows that the pressure in the cavity equilibrates on a time scale of some tens of ms. Panel (b) reveals that the maximum increase in the temperature of the gas is 20 and 50 K for the cases with 30 and 100 kPa, respectively, but also that the gas rapidly adopts the temperature of the cavity walls. More specifically, panel (c) illustrates that the decay is exponential with a time constant of 0.07 s for the case with 30 kPa and 0.14 s for 100 kPa. Since a process with an exponential decay will have decayed 6 orders of magnitude after 11 time constants, this implies that the average temperature of the center part of the cavity will rapidly (within a couple of seconds) decay to temperatures well within sub-mK of that of the cavity wall. For example, under atmospheric pressure conditions, the temperature of the gas will differ from that of the cavity wall only by 1 mK already after 1.5 s. This implies that the temperature difference between the wall and the center of the cavity will be negligible after the

initial part of a gas modulation cycle (in reality, after a couple of seconds). It also implies that the actual temperature of the gas at the cavity inlet is (for temperatures a few degrees around the working temperature) of practically no importance for the assessments; the temperature of the gas will still differ from that of the cavity wall by less than 1 mK already after a couple of seconds.

6.2. Gas-to-cavity-wall transfer of heat – heating of spacer

Despite the fact that the temperature of the gas in theory can increase up to some tens of percent of the absolute temperature when it is let into empty space (120 K for nitrogen) and, as shown by figure 4, some tens of K when let into a cavity of the dimensions of the system under study, figure 5 indicates that the maximum initial heating of the cavity walls will only be a small fraction of that of the gas (in this case only a couple of mK, i.e. four orders of magnitude smaller). This originates mainly from the fact that a solid material has a significantly higher volumetric heat capacity than a gas; e.g. the volumetric heat capacity of ULE-glass is $1.7 \times 10^6 \text{ J m}^{-3} \text{ K}^{-1}$ while it is $1.2 \times 10^3 \text{ J m}^{-3} \text{ K}^{-1}$ for nitrogen [33]. This is particularly emphasized when a metallic cavity is used since metals in general have higher volumetric heat capacity than glass; that of Invar is $4.3 \times 10^6 \text{ J m}^{-3} \text{ K}^{-1}$.⁵ Hence, although a gas can experience a significant increase in temperature when let into the cavity, its corresponding energy is only expected to give rise to a small temperature increase of the spacer material.

Of importance is also the amount of gas being brought into the refractometer by a gas filling. The Invar-based DFPC system scrutinized in this work only let $<5 \text{ cm}^3$ of gas into the system per filling. This implies that it brings in a minuscule amount of energy into the cavity spacer. Under atmospheric pressure conditions, this represents an energy of $<0.5 \text{ J}$. In contrast to conventional refractometry instrumentation, this only leads to a small temporary increase in the temperature of the walls of the cavity. For example, it is estimated that for the NIST FLOC system, for which 172 cm^3 of gas is let in in each filling, the gas brings in ca 17 J [17]. This implies that, for a given pressure, the amount of heat introduced into the Invar-based DFPC system is only 3% of that brought into the FLOC system. Furthermore, since the volumetric heat capacity of Invar is a few times larger than that of glass, a given amount of heat will produce a temperature increase in the Invar-based DFPC system that is a few times smaller than in a glass spacer (for the case with ULE-glass, 2.5 times smaller). It is therefore reasonable to assume that the momentary temperature increase in the Invar-based DFPC system should be at least two orders of magnitude smaller than what it is in the NIST FLOC system.

There is also a third reason why the maximum initial heating of the cavity walls in the Invar-based DFPC refractometer should be significantly smaller than those in many other types of refractometry systems, viz that the length scales in the

system are small. The energy brought into the cavity by the gas is proportional to the cavity volume, which in our case can be estimated as $\pi r^2 l$, where r and l are the radius and the length of the cavity, respectively. This energy is rapidly distributed over the cavity walls, whose area can be approximated by $2\pi r l$. This implies that the heat load on each wall area element scales with r , which, for the Invar-based DFPC system is small (only 3 mm, smaller than any other documented FPC-based refractometry system).

6.3. Thermalization of the cavity spacer

In order for the Invar-based DFPC refractometer utilizing the GAMOR methodology to assess the gas temperature accurately, it is also of importance that the transfer of heat in the system is fast. It should preferably be so swift that the energy supplied by the gas during the gas exchange processes does not give rise to any remaining spatial temperature inhomogeneity when the refractometry assessments are made.

The figures 5 and 6 illustrate that the diffusion of heat from the walls of the cavity into the spacer material takes place on approximately a ten second scale. It is shown that for the case with 30 kPa, the measurement cavity wall temperature has decreased (from a few mK) to sub-mK levels already after 10 s.

One reason for this fast heat diffusion is that the system is constructed without heat islands (i.e. with no internal isolation layers). This implies that the time scale of the heat propagation is predominantly governed by the thermal conductivity of the spacer material.

A second reason can be attributed to the fact that the cavity spacer is made of Invar, which has a ten times higher thermal conductivity than many types of glass (e.g. Invar has a thermal conductivity of $12\text{--}15 \text{ W m}^{-1} \text{ K}^{-1}$ [34] while ULE-glass has $1.3\text{--}1.4 \text{ W m}^{-1} \text{ K}^{-1}$ [33]) [25]. Hence, in an Invar-based DFPC any temperature inhomogeneity will dissipate one order of magnitude faster than it will in a glass-based one. This improves on the radial gradient of the temperature distribution in the cavity spacer and reduces significantly the time it takes for a given temperature change to level off to its steady state value.

After the heat has dissipated into the spacer (i.e. after some tens of seconds), the simulations (the figures 5 and 6) indicate that the temperature change of the spacer is in the sub-mK range. This is in agreement with the estimate of the maximum energy that is introduced by the gas. Since the heat capacity of the Invar cavity spacer is in the order of $1.7 \times 10^3 \text{ J K}^{-1}$, the maximum energy supplied by the gas (0.5 J) corresponds, assuming an even distribution of heat in the cavity spacer, to a temperature increase of only 0.3 mK. This is also favorable in comparison with the NIST FLOC system, in which the overall steady-state temperature rise after a gas filling was estimated to be one order of magnitude larger (3.4 mK) [17].

Moreover, since each gas filling is followed by a rapid gas evacuation process, in which a similar amount of energy is removed from the cavity (and thereby from the cavity spacer), the long-term net effect of the gas filling and evacuation process (comprising a number of gas filling and emptying

⁵ The volumetric heat capacity of the Invar-based DFPC system is $4260 \text{ J (l}^{-1} \text{ C}^{-1})$, calculated as the product of the specific heat [$520 \text{ J (kg}^{-1} \text{ K}^{-1})$] and the density (8.2 kg l^{-1}). The same entity for ULE glass (which is used in the NIST FLOC system) is $1690 \text{ J (l}^{-1} \text{ C}^{-1})$, calculated as the product of the specific heat [$767 \text{ J (kg}^{-1} \text{ K}^{-1})$] and the density (2.2 kg l^{-1}).

cycles) on the spatially averaged (steady-state) temperature of the cavity spacer is virtually null ($\ll 1$ mK).

6.4. Assessment of the temperature of the gas and its influence on the assessment of pressure

Since the Invar-based GAMOR system assesses the pressure from the molar density by use of a temperature measured by sensors placed in, or at the surface of, the cavity spacer, it is not significantly affected by any homogeneous heating of the cavity spacer; the system is only affected by a possible temperature gradient between the cavity wall and the positions in the spacer where the sensors are placed. Figure 7(b) illustrates that the difference in the temperature of the wall of the measurement cavity (which is assumed to be the same as that of the gas already after a couple of seconds) and that measured by the sensors (which is time-averaged over a few cycles) is on the sub-mK scale for large fractions of the gas modulation cycles. Thus, the temperature assessed by the sensors is a good representative of the actual temperature of the gas. Its uncertainty, which, for 100 s long modulation cycles, is 0.5 mK/100 kPa (1.8 ppm/100 kPa) and, for 200 s long cycles, 0.4 mK/100 kPa (1.3 ppm/100 kPa), also represents the uncertainty in pressure when pressure is assessed from refractivity.

It is additionally worth to emphasize that since the GAMOR methodology has the ability to eliminate the influence of the linear parts of drifts on its baseline (the signal from an empty measurement cavity), the linear part of any temperature drift of the spacer will not contribute to any offset or drifting baseline. The change of the temperature of the spacer from the pV -work during a modulation cycle, on the other hand, represents a non-linear type of drift that will affect an assessment of refractivity by changing the lengths of the cavities during the modulation cycle. However, since DFPC refractometry measures the change in the beat frequency between the two cavities, the assessed refractivity will be affected by such a temperature change of the spacer only if the lengths of the two cavities change dissimilarly. This will, in turn, take place only if the temperature of the two cavities changes dissimilarly, i.e. if the pV -work will change the temperature distribution in the spacer within the modulating cycle.

Panel (a) in figure 7 indicates that, during the last part of the filling section, the average temperature of the walls of the measurement cavity is about 100 μ K higher than that of the reference cavity while, during the last part of the evacuation section, it is 100 μ K lower. Since the coefficient of thermal expansion of Invar is in the order of 10^{-6} K^{-1} , a change of the temperature difference of the walls of the cavities of 200 μ K will lead to a change of the relative lengths of the two cavities (and thereby the refractivity) of (less than) 2×10^{-10} , which for 100 kPa of nitrogen corresponds to an error that is (smaller than) 0.7 ppm⁶.

⁶ Since the mirrors are in contact with the spacer at their rims, the change in mirror-to-mirror distance is given by the change in length of the spacer at some finite distances from the cavity walls at which the temperature differences are smaller than at the walls. This will therefore lead to a change in the difference in the lengths that is smaller than that at the walls of the cavities.

Since the change of the lengths of the cavities (< 0.7 ppm) will produce an effect on the refractivity that has opposite sign to that of the change of the gas temperature (estimated to 1.3 ppm/100 kPa), both for a 200 s long modulation cycle, the real uncertainties will be smaller than latter, given by the difference of the two.

6.5. Experimental assessments

The conclusions above are in good agreement with experiment results. The panels (b), (d), (f), and (h) in figure 8 show that the temperature is virtually constant during the gas filling-and-settling process; the measurements do not show (within their levels of noise), for any pressure, any temperature dependence that can be attributed to any type of modulation-induced temperature variation. We interpret this as there is no influence of pV -work on the temperature of the gas at the time in the modulation cycle when the refractivity assessments are made, which is after 40 (or 90) s⁷.

The panels (a), (c), (e), and (g) in the same figure show that the reproducibility of the assessment of pressure between individual gas filling cycles (i.e. the precision) are, for each pressure, better than their short-term noise. This indicates that the assessments, and in particular their averages (the black solid curves), are trustworthy assessments of the pressure in the cavity during the filling-and-stabilization process. Since the dashed horizontal lines represent ± 3 ppm, these curves indicate that their variations during the last 75 s of the filling-and-stabilization period are all in the low ppm range; they drift slightly (less than 1 ppm) over the measurement time, with a slowly increasing pressure with time. There can be at least three possible explanations for this trend, viz: (i) a drifting temperature; (ii) a drifting molar density; or (iii) a drifting length of the cavity. A comparison with the data in the panels (b), (d), (f), and (h) indicates that it is improbable that the variations are due to drifts in the temperature. It is also improbable that it is due to a drifting cavity length since the interpolation process that takes place in the GAMOR methodology eliminates the influence of the linear part of drifts (in theory, it could be due to a non-linear drift that is not eliminated by the GAMOR methodology [19]). It was instead assumed that this was caused by a drift in the pressure provided by the DWPG (related to the height of the piston). Since it has previously been noticed that the pressure created by a DWPG can have a weak dependence on the height of the piston [35], it is plausible that the observed effect has this origin. Further investigation of this phenomenon will be undertaken in future studies.

All this indicates that the presented Invar-based DFPC system is significantly less affected by thermodynamic effects related to the gas exchange process than the NIST FLOC system. In fact, such effects should be virtually negligible (in the

⁷ If the cycle-resolved experimental results had indicated a detectable amount of modulation-correlated effects, they could have been attributed to either the refractometry or the DWPG. However, since the data do not show evidence of any such effects, it is possible to conclude that neither the refractometry, nor the DWPG, give rise to any modulation-correlated temperature variations in the system and that the system therefore is not affected noticeably by any pV -work.

sub-mK range) despite the use of gas modulation cycle times of 100 s, as is the case when using the GAMOR method.

7. Conclusion

This work has presented a detailed scrutiny of the influence of the gas exchange process on the assessment of gas temperature (and thereby pressure) on the Invar-based dual-Fabry–Pérot cavity (DFPC) instrumentation used with the GAMOR methodology [15, 25, 26]. Simulations show that the equilibration of pressure in the cavity when nitrogen is let in takes place on a time scale of ten milliseconds and that the gas adopts the temperature of the cavity wall on a time scale of less than a couple of seconds.

Since the cavity volume is small ($<5 \text{ cm}^3$), the gas transfers only a small amount of energy ($<0.5 \text{ J}$) into the system during the gas filling process. This will give rise to only a minor local heating of the cavity spacer. Because of the fact that the system is constructed without heat islands and due to the large thermal conductivity of Invar (one order of magnitude larger than for typical glasses), this minor local heating will rapidly dissipate into the material.

Moreover, since the system assesses temperature by the use of sensors placed either in holes drilled in the cavity spacer or wrapped tightly around the outside of the spacer, any possible homogeneous heating of the cavity spacer affecting the gas temperature (and thus the pressure assessments) can be measured and will directly be accounted for. Therefore, the pressure assessments are only influenced by the difference between the temperature of the cavity walls and that of the cavity spacer at the position(s) of the sensors. It was found that, under normal conditions (for pressures up to 100 kPa and when the gas modulation times are 100 or 200 s), this difference will, when the refractivity assessments are made, only be in the sub-mK range.

It has been estimated that an upper limit for the influence of pV -work made by nitrogen on the Invar-based DFPC system, is, for 100 s long modulation cycles, 0.5 mK/100 kPa (or 1.8 ppm/100 kPa) and, for 200 s long cycles, 0.4 mK/100 kPa (or 1.3 ppm/100 kPa). These estimates were compared with experiments performed in the 4–30 kPa range. Since none of these assessment showed any resolvable effect from pV -work, they support the estimates.

Simulations analogous to those of the heat exchange of nitrogen with the walls were performed also for argon and helium (although not shown above). It was found that for argon, the heat exchange takes place on the same time scale as for nitrogen, while for helium, it is (significantly) faster. Hence, the conclusion that the pV -work has a negligible effect on the temperature of the cavity walls when the filled measurement cavity assessments are made can be extended also to these gases.


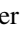
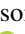



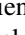




Currently, the lowest expanded measurement uncertainty ($k = 2$) reported for an Invar-based dual-Fabry–Pérot cavity system is $[(10 \text{ mPa})^2 + (10 \times 10^{-6} p)^2]^{1/2}$ [15]. This implies that thermodynamic effects of gas exchanges (pV -work) are currently not a limiting factor when the Invar-based DFPC

GAMOR system is used for assessments of pressure or as a primary pressure standard up to atmospheric pressure.

Acknowledgments

This project (QuantumPascal, 18SIB04) has received funding from the EMPIR programme co-financed by the Participating States and from the European Union's Horizon 2020 research and innovation programme; Vetenskapsrådet (VR) (621-2015-04374 and 621-2020-05105); the Umeå University Industrial doctoral school; the Vinnova Metrology Programme (2017-05013, 2018-04570, and 2019-05029); the Kempe Foundations (1823.U12).

ORCID iDs

T Rubin  <https://orcid.org/0000-0002-6794-5071>
 I Silander  <https://orcid.org/0000-0001-5790-2185>
 J Zakrisson  <https://orcid.org/0000-0002-3261-9903>
 M Hao  <https://orcid.org/0000-0001-6113-6719>
 C Forssén  <https://orcid.org/0000-0001-6824-3111>
 P Asbahr  <https://orcid.org/0000-0001-9383-1353>
 M Bernien  <https://orcid.org/0000-0002-1734-1800>
 A Kussicke  <https://orcid.org/0000-0002-3466-381X>
 K Liu  <https://orcid.org/0000-0003-0542-1739>
 M Zelan  <https://orcid.org/0000-0001-9068-6031>
 O Axner  <https://orcid.org/0000-0002-8580-9700>

References

- [1] Andersson M, Eliasson L and Pendrill L R 1987 *Appl. Opt.* **26** 4835
- [2] Fang H, Picard A and Juncar P 2002 *Rev. Sci. Instrum.* **73** 1934
- [3] Pendrill L R 2004 *Metrologia* **41** 40
- [4] Egan P and Stone J A 2011 *Appl. Opt.* **50** 3076
- [5] Mari D, Bergoglio M, Pisani M and Zucco M 2014 *Meas. Sci. Technol.* **25** 125303
- [6] Takei Y, Arai K, Yoshida H, Bitou Y, Telada S and Kobata T 2020 *Measurement* **151** 107090
- [7] Axner O, Silander I, Forssén C, Zakrisson J and Zelan M 2021 *Spectrochim. Acta B* **179** 106121
- [8] Buckingham A D and Graham C 1974 *Proc. R. Soc. A* **337** 275
- [9] Jaeschke M, Hinze H M, Achtermann H J and Magnus G 1991 *Fluid Phase Equilib.* **62** 115–39
- [10] Achtermann H J, Magnus G and Bose T K 1991 *J. Chem. Phys.* **94** 5669
- [11] Egan P F, Stone J A, Hendricks J H, Ricker J E, Scace G E and Strouse G F 2015 *Opt. Lett.* **40** 3945
- [12] Egan P F, Stone J A, Ricker J E and Hendricks J H 2016 *Rev. Sci. Instrum.* **87** 053113
- [13] Jousten K et al 2017 *Metrologia* **54** 146
- [14] Silvestri Z, Boineau F, Otal P and Wallerand J P 2018 *CPEM 2018—Conf. on Precision Electromagnetic Measurements* pp 14–5
- [15] Silander I, Forssén C, Zakrisson J, Zelan M and Axner O 2021 *J. Vac. Sci. Technol. B* **39** 044201
- [16] Yang Y, Rubin T and Sun J 2021 *Vacuum* **194** 110598
- [17] Ricker J, Douglass K O, Syssoev S, Stone J, Avdiaj S and Hendricks J H 2021 *Metrologia* **58** 035003
- [18] Avdiaj S, Yang Y, Jousten K and Rubin T 2018 *J. Chem. Phys.* **148** 116101

- [19] Axner O, Forssén C, Silander I, Zakrisson J and Zelan M 2021 *J. Opt. Soc. Am. B* **38** 2419
- [20] Silander I, Hausmaninger T, Zelan M and Axner O 2018 *J. Vac. Sci. Technol. A* **36** 03E105
- [21] Silander I, Hausmaninger T, Forssén C, Zelan M and Axner O 2019 *J. Vac. Sci. Technol. B* **37** 042901
- [22] Zelan M, Silander I, Forssén C, Zakrisson J and Axner O 2020 *Acta IMEKO* **9** 299
- [23] Forssén C, Silander I, Szabo D, Jönsson G, Bjerling M, Hausmaninger T, Axner O and Zelan M 2020 *Acta IMEKO* **9** 287
- [24] Forssén C, Silander I, Zakrisson J, Axner O and Zelan M 2021 *Sensors* **21** 6272
- [25] Silander I, Forssén C, Zakrisson J, Zelan M and Axner O 2020 *Opt. Lett.* **45** 2652
- [26] Silander I, Forssén C, Zakrisson J, Zelan M and Axner O 2020 *Acta IMEKO* **9** 293
- [27] Baker B 1999 *Am. J. Phys.* **67** 712
- [28] Jousten K 1994 *Vacuum* **45** 1205
- [29] Zakrisson J, Silander I, Forssén C, Zelan M and Axner O 2020 *J. Vac. Sci. Technol. B* **38** 054202
- [30] Puchalski M, Piszczatowski K, Komasa J, Jeziorski B and Szalewicz K 2016 *Phys. Rev. A* **93** 032515
- [31] Axner O, Silander I, Hausmaninger T and Zelan M 2017 arXiv:1704.01187v2
- [32] Forssén C, Silander I, Zakrisson J, Axner O and Zelan M 2022 An optical Pascal in Sweden *J. Opt.* **24** 033002
- [33] Corning inc. 2016 *Ultra Low Expansion Glass - ULE® Corning Code 7972* <https://www.corning.com/media/worldwide/csm/documents/7f674d33bf65415991f66861245349d32.pdf>
- [34] AZoMaterials 2001 *Invar - Nickel Iron Alloy* <https://azom.com/properties.aspx?ArticleID=515>
- [35] Jain K, Bowers W and Schmidt J W 2003 *J. Res. Natl Inst. Stand. Technol.* **108** 135